PULLOUT INTERACTION MECHANISM OF SQUARE SHAPED GEOCELL REINFORCEMENT IN SAND

Kelum SENEVIRATHNA[1], Henry MUNOZ[2], Takashi KIYOTA[3] and Toshihiko KATAGIRI[4]

ABSTRACT: The influence of the spacing of the transverse members of square-shaped geocell reinforcements embedded in sand was investigated on the pull-out resistance of the composite reinforcement-backfill. In addition, the deformation patterns of the composite were examined by a non-contact measurement technique via digital image correlation analyses to shed lights into the plausible interaction mechanism of the reinforcement-sand. The pull-out tests were carried out under plane-strain condition with the geocell reinforcements having a spacing of 180 mm, 90 mm and 30 mm while their transversal member height as well as their longitudinal length and height were constant for consistent comparison. It was found that the interaction between sand backfill and reinforcement is dependent on the spacing of the transverse member, i.e. by either ratio spacing/height of the reinforcement (ST/HT) or spacing/grain size (ST/D_{50}). As ST/HT increases, the pull-out failure of the composite falls into three different failure modes, from brittle failure, intermediate failure to more ductile failure. There was identified that the ductile failure type was associated to a lower pre-peak stiffness and lower peak pull-out resistance of the composite. On the other hand, brittle and intermediate failures were associated to higher values of pre-peak stiffness and so peak pull-out resistance. The deformation of the composite confirm different patterns associated with these three different failure types.

Key Words: Geocell, interaction mechanism, pull-out deformation, Digital Image Correlation

INTRODUCTION

Geosynthetic-reinforced soil retaining walls (GRS) with full height rigid (FHR) facing have become far popular in Japan since the past few decades for the construction of GRS retaining walls (RW) and GRS integral bridges (IB) due to the high seismic performance and low construction cost of these structures (Munoz et al. 2012, Tatsuoka et al., 2014). Usually geogrids, as planar tensile reinforcements, are used for reinforcing a GRS backfill made of high quality soil. Nonetheless, large particles and poorly graded soils can commonly be found available for backfilling and they might not be able to interact efficiently with geogrids to reinforce and enhance the strength of a poorly graded soil so to make a GRS backfill sufficiently strong to perform adequately under high seismic demands. In this view, geocell reinforcement has become an alternative to reinforce soils with large particles. However, it was found that the conventional type geocell reinforcements (i.e. diamond shaped geocells), which is typically used to reinforced soft soils against vertical load demands, have low tensile strength and stiffness. Hence, they are weak to act effectively as reinforcement for the backfill of GRS RW and GRS IB to sustain lateral load demands for medium to severe earthquakes (Kiyota et

[1] MSc Student, Department of Civil Engineering, University of Tokyo
[2] Post-Doctoral Researcher, Institute of Industrial Science, University of Tokyo
[3] Associate Professor, Institute of Industrial Science, University of Tokyo
[4] Technical Director, Institute of Industrial Science, University of Tokyo

al., 2009).
In this view, new types of square shaped geocells are being developed at the Institute of Industrial Science (IIS) of the University of Tokyo. The new type of reinforcements have shown a potential with increasing their performance when compared to the conventional diamond type geocell. This is attained by firstly, having the geocell made of longitudinal and transversal members connected perpendicular to each other, and secondly, by promoting a more efficient confinement of large soil particles within individual cells, in turn the composite geocell-soil can mobilised a higher frictional and anchorage resistant capacity that act against pull out demands.
The interaction mechanism of square shaped geocell reinforcements with the backfill and the associated failure mechanism are not well understood yet. This interaction depends on several factors related to the reinforcement including height (HT) and spacing (ST) of transverse members, backfill particle size (D_{50}), degree of compaction (D_C), and others. The spacing of the transversal members ST plays an important role in the failure modes of the composite reinforcement-backfill, which needs further study. The latter is the objective of this paper.
A practical and effective tool for quantitative in-plane deformation measurement of an object surface can be achieved by non-contact measurement techniques via the application of digital image correlation (DIC). DIC can provide the field deformations of an object and thus shed insights into plausible failure modes when the object is subject to external loads (Munoz et al., 2016a,b, Munoz et al., 2017a,b).
Based on the above background, the aim of this study is to investigate the pull-out interaction, failure modes and a plausible pull-out failure mechanism of the composite sand-square shaped geocell reinforcement.

TESTING APPARATUS, MATERIALS AND PROCEDURES

Pullout test apparatus and DIC set up

The set up of the pull-out apparatus and box with the reinforced sand is presented in Figure 1a and b. The pull-out apparatus was developed at the IIS, the University of Tokyo. The pull-out tests were carried out under plane-strain condition. The pull-out box was made of wood and had an acrylic window in the front which was useful to observe the deformation of the backfill via image analyses and tracking deformed subsets. The inner dimensions of the box are 500mm (length) × 400mm (height) × 150mm (width). The box has an opening in its transversal left side to allow passing through the extensions of reinforcement that is resting in the sand inside the box so the reinforcement head can be connected to the pull-out gear, see Figure 1a. The opening of the box was fixed to 60 mm. After laying down the reinforcement in the sand, the opening was sealed with soft sponge to avoid any sand spilling during subsequent filling of the box.

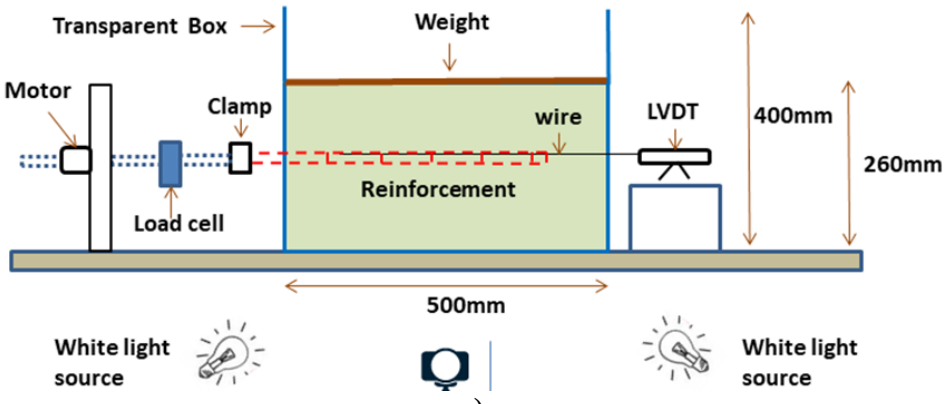

a)

Figure 1: a) Schematic set up of the pullout testing

To undertake digital image correlation (DIC) analyses on the backfill deformations, a high-speed camera was set up on a platform that was designed to be adjustable to any height and distance relative to the box so that to have the camera pointing exactly perpendicular onto the acrylic window of the box. Under this set up, it was possible to capture pictures of a prescribed area of interest. Two white light sources were set up an angled pointing towards the acrylic window of the box to supply uniform lighting during the test, which is important for acquiring a high-quality image for later analyses. A picture of the DIC setup is presented in Figure 1b. A similar set up with DIC has been previously implemented and described by Munoz et al. (2006a, b).

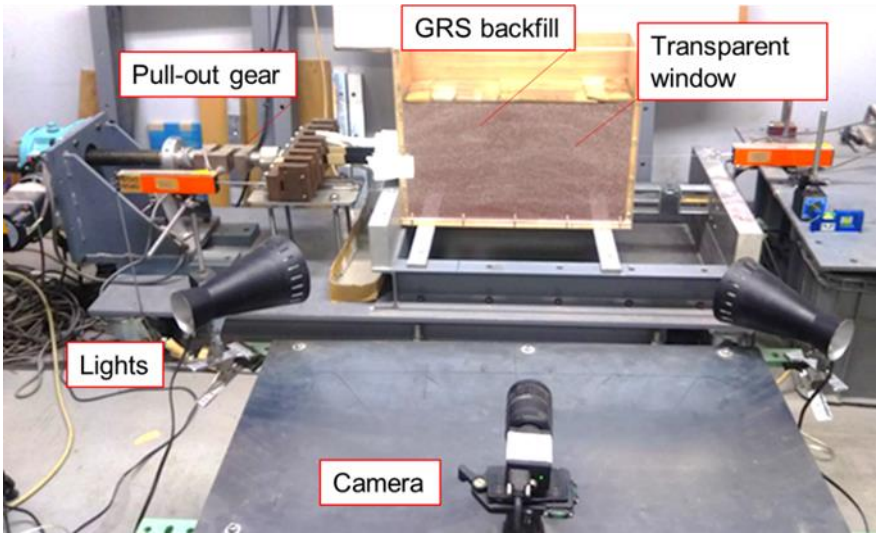

b)

Figure 1: b) a picture of the pullout testing set up

Geocell reinforcement model

The square shaped geocell reinforcement consists of cells formed by the arrangement of a series of straight longitudinal members (LM) and transversal members (TM) at a prescribed spacing (S). Figure 2 shows the square shaped geocell reinforcement used in the present study. The LMs were made of flexible polyethylene stripes (longitudinal members height of HL=18.75 mm), while rigid metal strips made of aluminum formed the (transversal members HT=12.5 mm). The LM are tensile strong enough and they did not experience tensile breakage at any moment, so pull-out failure dominated the models geocell-sand.

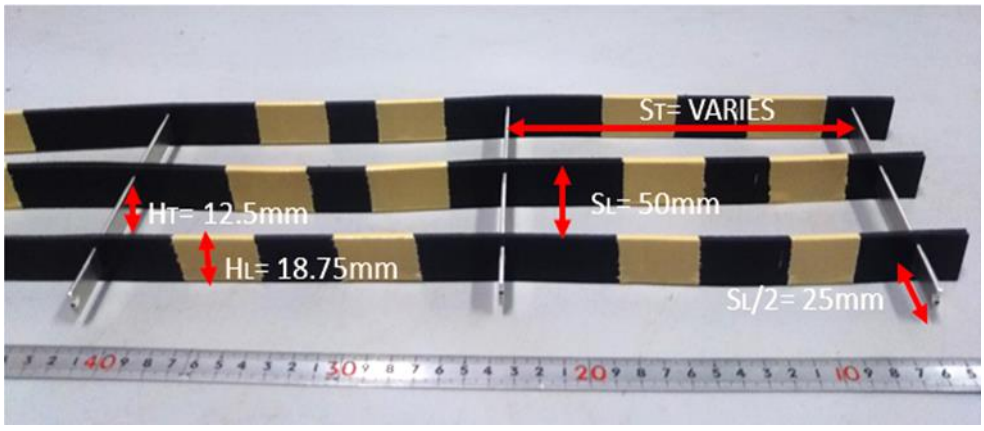

Figure 2 Square shaped geocell reinforcement used in the study

The spacing between LMs (SL= 50 mm) was kept constant in all the reinforcements, while the spacing between TMs (ST) varied for three spacing ST of 30 mm, 90 mm, and 180 mm to study the effects of ST on the pull out response and associated failure modes during the tests. The size of the each geocell mattress was 360 mm (length) and 125 mm (width) to fit the geocell within the testing box. To allow free movement of the sand within the cells in contact with the acrylic window of the testing box, a separation of (SL/2) between the window and the immediate longitudinal member was anticipated. This allows successfully capturing the deformations of the backfill inside the cells by the DIC method, which was deemed representative of the deformation of the models. A distance of 70 mm was kept constant between the left side of the wall of the box and the first TM of the geocell.

Testing Procedure

Poorly graded sub-rounded Silica sand (D_{50} of 0.25 mm and friction angle of 34 degrees) was poured into the box and then compacted in 50 mm thick sub layers making a total of a 260 mm backfill height. The geocell reinforcement was embedded in the middle level of the backfill. The target density of the backfill was 1.53 g/cm^3 considering a nearly 100% degree of compaction. Led shot bags were placed in the crest of the backfill to increase the vertical stress in the existing sand by 1 kPa (i.e. the total vertical stress acting on the reinforcement about 2.5 kPa).

Horizontal displacement of the first transversal member of the geocell TM (results are not presented herein) was measured by a extensometer made of inextensible wire connected to a Linear Variable Displacement Transducers (LVDT) located in the gear of the box, as shown in Figure 1a and b. In addition, the horizontal displacement (results of D0 and D are not presented herein) of the clamp (in the pull-out gear) was measured with a LVDT. The pull out force was applied to a rate of 2.5mm/min. The pull-out force was measured by a load cell with capacity of 49 kN ± 98 N at a frequency of 1 Hz, i.e. a data point per second.

The digital images were taken by a high-speed camera at a same frequency of 1 Hz for one to one correspondence of load-deformation. The natural white-coloured Silica sand was mixed with a dyed-in-red Silica sand (50% ratio) in order to obtain a speckle-like pattern of the backfill. DIC measurements rely on a non-repetitive, high contrast speckle pattern of the object under measure (Munoz et al. 2016a, b, Munoz et al 2017a, b). With this mixture, it was ensured a good pattern for the anticipated DIC measurements. For the DIC analyses, a subset of 40 x 40 pixels was used in the form of point components to track deformations. An example of the image of the area of interest of the backfill acquired and analysed applying DIC for the resulting displacement vectors of the deformed backfill are shown in Figure 3.

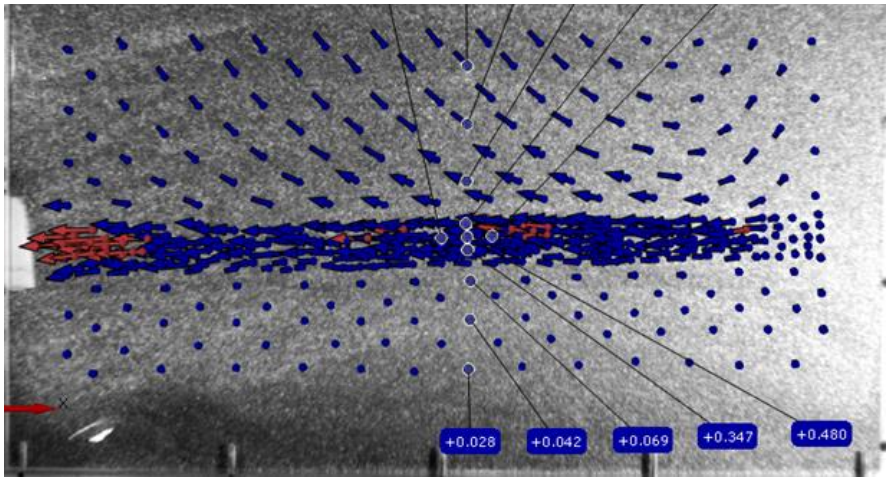

Figure 3 A grey scale picture of the backfill and DIC vector of displacements in the backfill

TESTING PROGRAM

This study was focused on identifying the effects of the spacing of the transversal members of the geocell (ST) on the pull out response, deformations of the backfill and failure mechanism. Hence, ST varied as indicated in Table 1, while other geometrical parameters of the geocell such as SL, HL, HT shown in Figure 2 were kept constant. In addition, the backfill material and its density were kept constant in the tests (i.e. D_{50}= 0.25 mm, D_C=100% and vertical stress of 2.5 kPa).
Three testing cases were performed as presented in Table 1. DIC measurement was performed in each test.

Table 1: Testing program cases

No.	Legend reference	Spacing (ST)	ST/HT	ST/D_{50}	Transverse members
1.	S180	180 mm	14	720	3
2.	S90	90 mm	7	360	5
3.	S30	30 mm	3	120	13

RESULTS AND DISCUSSION

Time history of pull-out resistance
The time history of pull-out resistance (PR) of the tests described in Table 1 is presented in Figure 4. The pull-out results from the tests are summarised in the Table 2. Further analyses on the pull-out response with the reinforcements suggest that the response can be attributed to the extent of the following resisting components against the pull-out force, including: 1) the mobilised shear stress along the interface between the sand inside the cells and immediate surrounding backfill; and 2) the increase in the passive resistance in each cell provided by the confined sand inside each cell in immediate contact with the transversal members.

Table 2: Summarised results for the tests

Geocell	Pre peak stiffness	Peak PR (KN/m)	Residual PR (KN/m)	Failure mode
S180	Low	3.0	2.5	Ductile
S90	Moderate to high	3.6	2.0	Intermediate
S30	High	3.4	2.0	Brittle

The results in Figure 4 show that with S180 a peak pull-out resistance was attained at 3 kN/m. In this case, the response curve shows a plateau-like featuring the pull-out peak regime. After peak during the post-peak regime, the PR curve softened slightly and a pullout strength of 2.5 kN/m was recorded. This behaviour corresponds to a pull-out ductile failure.
The pull-out response with S180, with S/H of 14, can be attributed to the increase of resisting components 1 and 2 explained above until peak resistance took place. Thereafter, it can be speculated that the passive resistance, component 2, may have decreased significantly, as active displacement of the TM took place inducing the loosening of the sand immediately behind the TM and thus making the backfill inside the cells loose and weak which did not contribute to a higher resisting component 2. In similar fashion, component 1 may have decreased due to the loss of the effective contact of soil particles due to active settlements of the sand and the loosening of the backfill.
A more pronounced decreased in the peak pull-out resistance was observed with S30 and S90, as number of members of TM increased between 5 to 13, i.e. S/T= 3. Similarly as above, shear stress and passive resistance were mobilised in these cases.
With S90, there was an additional increase in pre-peak stiffness and PR to 3.6 kN/m. This can be attributed mainly to the increase in the passive resistance in the cells as a result of having the sand inside the cell confined more effectively than with S180 as a result of using a shorter spacing S/H of 7.

A similar peak PR was observed with S30, S/T= 3, equal to 3.4 kN/m.
Although the peak PR with S90 and S30 were nearly the same, i.e. peak PR of 3.6 and 3.4 kN/m, respectively, their pre-peak and post-peak behaviour were markedly different. In pre peak regime, the stiffness with S30 was higher than with S90. In post-peak regime, with S30 it was showed a more abrupt fashion in the decreased of the resistance (i.e. softening) after peak PR took place when compared with S90. The failure mode with S30 is a typical failure of more rigid materials or systems. Hence, this failure was referred to as brittle-type failure. With S90, the failure mode was deemed in between ductile to brittle.

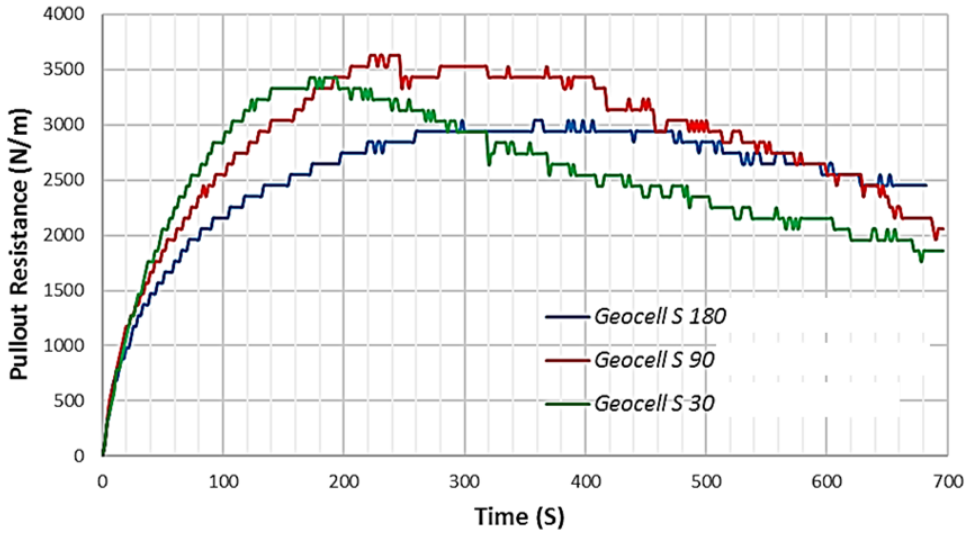

Figure 4: Pull-out resistance against time for the test

Deformation patterns in the backfill and failure modes
Figures 5 to 7 show the deformation patterns of the backfill obtained from DIC analyses. These figures correspond to the deformations at peak and residual states. The magnitude of displacement vectors, can be observed in the colour legend in these figures.
An important feature provided by these figures is that deformation (and does failure) takes place only in upper levels in the backfill from the bottom of the geocell, so that a non-symmetrical deformations respect to the x-axis characterised the models. Hence, it is demonstrated that the pull-out failure behaviour of a geocell reinforcement might not be characterised using approaches of failure mode for rigid grids (e.g. Bergado, 1996).
The following failures modes were observed from the displacement analysis:

a) Ductile failure mode
This type of failure took place with S180. The deformation pattern of the composite at the peak and residual states are shown in Figure 5a and b, respectively. The vector of displacements indicate the deformation pattern was composed by of both a wing-type and a bulb-type. The wing-type deformation pattern suggests that the sand in front the TM move upwards induced by the pull-out force in the reinforcement and due to the effects of dilatancy of the sand a shear stress mobilises in the interface between the sand inside the cells and the surrounding backfill. Hence, the development of this wing is constrained by the vertical stress by the weight of the sand.
In addition, a bulb-type deformation pattern can be attributed to the active displacements of the TMs which induced settlements of the sand immediately behind the TMs (e.g. see the downwards vectors in Figure 5). In turn, the sand inside the cells loosened which may have result in a decreasing effect in the passive resistance. The passive resistant component acts against the pull-out force, hence a decrease in this component induced a lower pull-out resistance response. Therefore, this is indicative that the

separation of the TMs, ST of 180 mm, was relatively large so the cells were not able to confine effectively the sand.
Deformations vector also developed along the interface, in between the sand inside the cells in contact with the immediate backfill, at both bottom and top of the geocell reinforcement (see the horizontal vectors in this interface in Figure 5). In turn shear stress was mobilised that acted as a resisting component against pull-out demands.
Figure 5 also shows the displacement of the sand along adjacent TMs. The displacement vector suggest the deformations took place in a progressive and delaying fashion with time (i.e. deformations were not mobilised simultaneously) due to a relative large ST of 180 mm. This type of behaviour has been noted by Kiyota et al. (2009) for flexible reinforcements (i.e. unlike a rigid-like deformation behaviour typical of geogrids). This is an indication that the applied pull-out force was not transferred effectively all along the reinforcement.

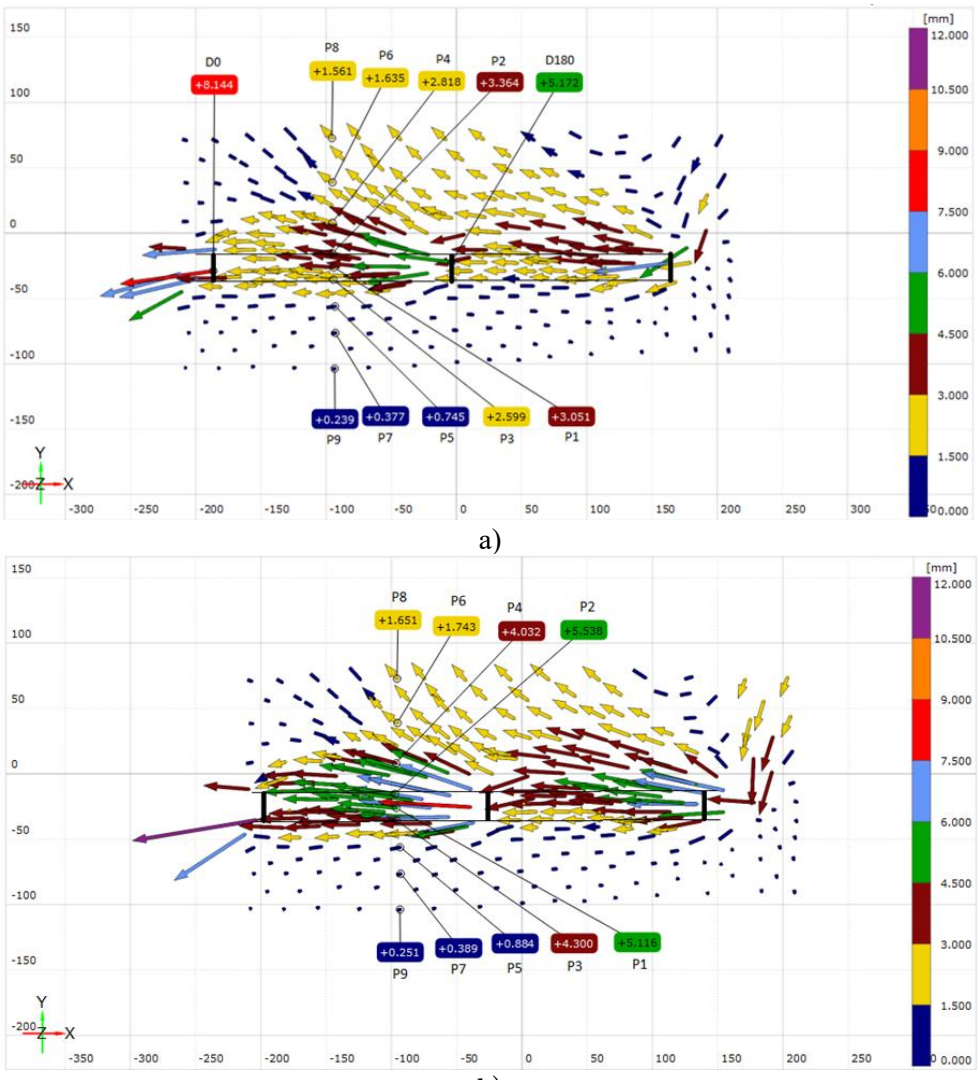

Figure 5: Deformation pattern with S180 at a) the peak and b) residual state

b) Intermediate ductile-to-brittle failure mode
This type of failure took place with S90. The curve characteristic of this failure is shown in Figure 4. The deformation pattern of the backfill is show in Figure 6a and b at the peak and residual state, respectively. Similarly as described above, deformations took place on the upper layer from the bottom

of the reinforcement. With S90, the bulb-type failure that was typical with S180 was not formed, rather a single wing-type deformation pattern was formed. This can be attributed to several factor including, but not limited to, the following: 1) a smaller separation of the transversal members that confined more effectively the sand inside the cells. 2) The pull-out force was distributed and activated nearly simultaneously along the reinforcement, so active displacement of the TM took place in a lesser extent, if not eliminated, and 3) as a result of factor 2, active settlements, if any, took place in a lesser extent
In addition, factors 1 and 2 seem that characterised the deformation pattern by providing a nearly same magnitude of displacement vectors in the sand inside the cells as shown in Figure 6. Factor 3 was influential in the consistent upward displacement of the backfill along the cells that form a wing-type deformation pattern at any time. The above factors overall confined the sand more effectively and therefore the passive resistance was kept higher.

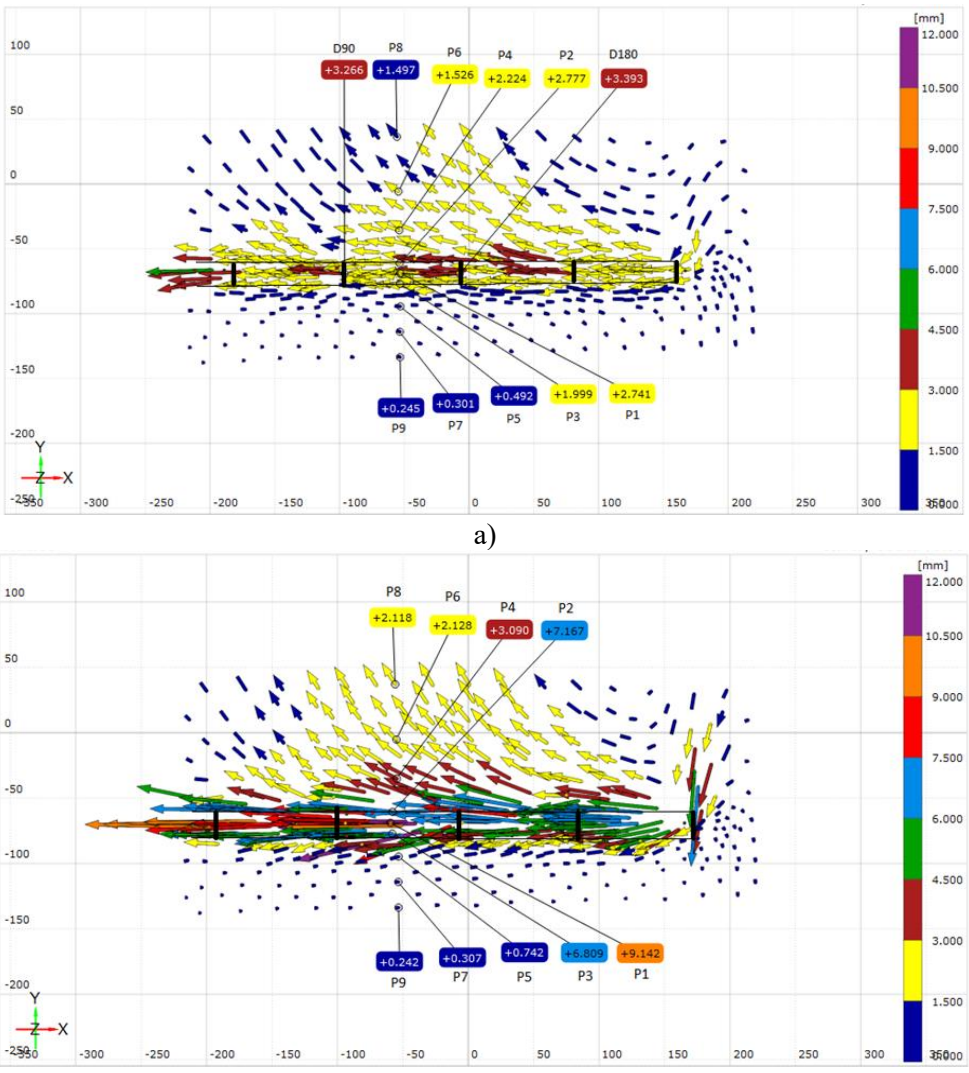

Figure 6: Deformation pattern with S90 at a) the peak and b) residual state

c) Brittle failure mode

A brittle type failure occurred with S30. Figure 4 shows the pull-out resistance curve with S30. The deformation pattern of the backfill with S30 at the peak and residual state are shown in Figure 7a and b, respectively.
With S30, the vector of displacements in the cells seems that developed far more uniformly and nearly

simultaneously in comparison with S180. Hence, the reinforcement together with the sand inside its cells seems to behave monolithically. This behaviour was positive in the overall pull-out response, i.e. with this reinforcement, the highest pre-peak stiffness was obtained, a higher pull-out resistance was attained (3.4. kN) , and the deformation of the backfill were restrain more effectively in contrast to S90 and S180, e.g. see the magnitude of vector displacement in the wing-type deformation in Figures 4, 5 and 6. However, after peak resistance took place, the pull-out failure took place in a more brittle fashion, i.e. the resistance was lost quicker and in abrupt fashion, unlike with S90 and S180.
Thus, with S30, although a relatively high pre-peak stiffness and pull-out strength are relevant to GRS structures to sustain higher pull-out demands under limited deformations, an abrupt failure may be undesirable with such structures.

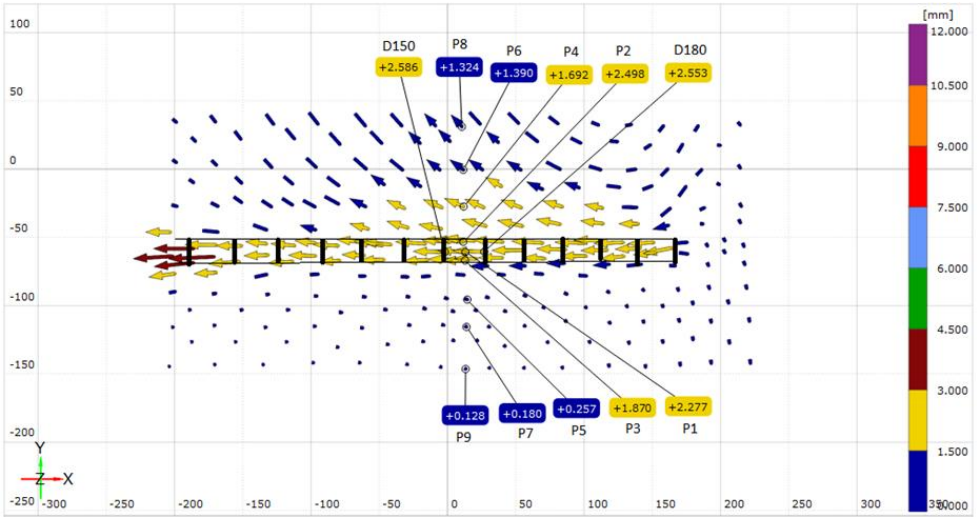

a)

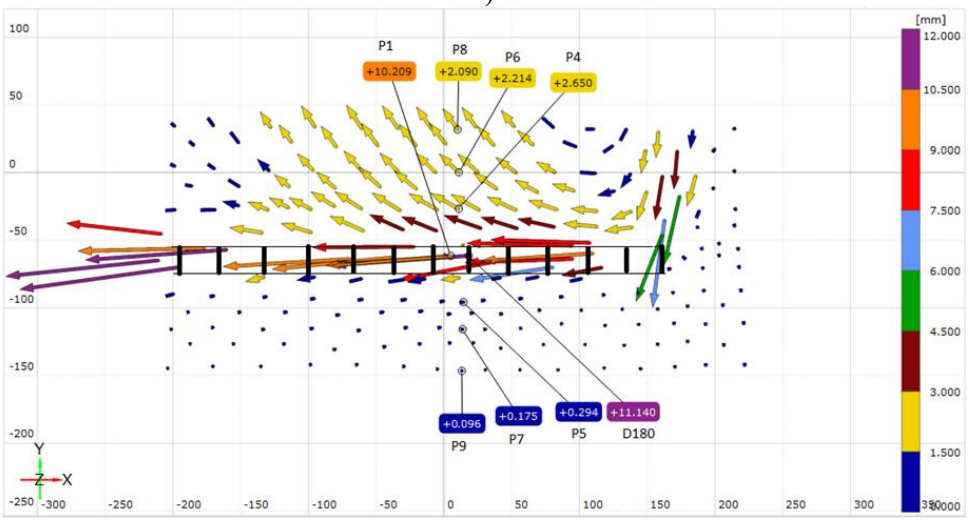

b)

Figure 7: Deformation pattern with S30 at a) the peak and b) residual state

Threshold limits for failure modes

The results presented above indicate that the interaction between the backfill and the reinforcement is dependent on S, i.e. either by the ratio ST/HT or ST/D_{50}, which has resulted into three types of failure, i.e. ductile, intermediate and brittle failure with ST/HT of 3, 7, and 14, (ST/D_{50}= 720, 360, 120), respectively. The results of the peak PR versus ST/HT is presented in Figure 8. From this figure the following features can be drawn:

The peak PR with S30 (ST/HT= 3) and S90 (ST/HT= 7) attained nearly the same strength of 3.4 kN/m and 3.6 kN/m, only 6% of difference. With S30, the failure was more brittle. With S90, the model failure of the composite was in between from brittle towards ductile. The peak PR with S180 (ST/HT= 14) attained a lower strength of 3.0 kN/m, 83% lower than S90, and the pull-out failure was more ductile.

The enveloped of the peak PRs in Figure 8 suggests that additional testing with ST/HT in between 3 and 7 would be needed to define a plausible threshold that separates brittle to intermediate failure. In this same manner, further testing with ST/HT > 15 would be required to define a lower bound of ST/HT associated to a fully ductile failure. However, for GRS RW and GRS IB applications, which requires the GRS backfill stiffer and strong, ST/HT between 3 and 7 may be of greater interest.

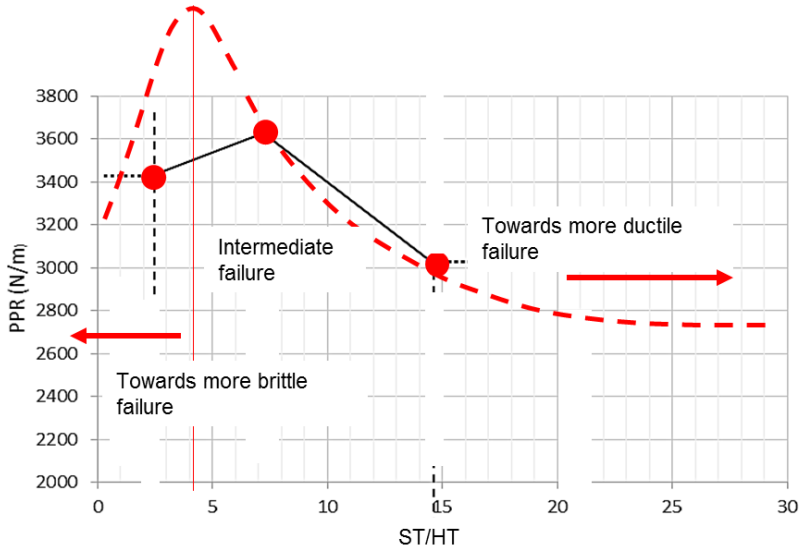

Figure 8: Failure modes with different ST/HT

CONCLUSIONS

The study focused on identifying the pull-out response and plausible failure modes with square shaped geocell reinforcements embedded in sand. The effect of increasing the spacing of the transversal members of the reinforcement were examined on the failure modes of the reinforcement-sand composite. It was found that upon the increase of the spacing of the transversal from by the ratio ST/HT from 3, 7 and 14 (ST/D_{50}= 120, 360, 720), brittle, intermediate and ductile-type failure modes were obtained, respectively. In addition, the deformation patters associated to these failure modes were obtained by using a non-contact measurement technique via digital image correlation. This technique allows to extracting deformations of an object from a series of images via pattern tracking algorithms. The deformation of the composite confirm different patterns associated with these the failure.

REFERENCES

Bergado D. T, Chai J. C, Miura N. (1996). Prediction of pullout resistance and pullout force-displacement relationship for inextensible grid reinforcements. Soils and foundations, 36(4): 11-22.

Kiyota, T., Soma, R., Munoz, H., Kuroda, T., Ohta, J., Harata, M. and Tatsuoka, F. (2009). Pullout behaviour of geocell placed as reinforcement in backfill, Geosynthetics Engineering Journal 24(0), 75-82. (In Japanese).

Munoz H, Taheri A. & Chanda E. (2016a). Fracture energy-based brittleness index development and brit-tleness quantification by pre-peak strength parameters in rock uniaxial compression. Rock Mechanics and Rock Engineering, 49 (12): 4587–4606.
Munoz H, Taheri A. & Chanda E. (2016b). Pre-peak and post-peak rock strain characteristics during uniaxial compression by 3D digital image correlation. Rock Mechanics and Rock Engineering, 49 (7): 2541–2554.
Munoz H, Taheri A. &, Chanda E. (2017a). Local damage and progressive localisation in porous sandstone. Rock Mechanics and Rock Engineering, 50 (1): 3253–3259.
Munoz H, Taheri A. &, Chanda E. (2017b). Specimen aspect ratio and progressive field strain development of sandstone under uniaxial compression by three-dimensional digital image correlation. Journal of Rock Mechanics and Geotechnical Engineering, 9 (1): 599-610.
Munoz H, Tatsuoka F, Hirakawa D, Nishikiori H, Soma R, Tateyama M & Watanabe K.(2012). Dynamic stability of geosynthetic-reinforced soil integral bridge. Geosynthetics International, 19 (1): 11-38.
Tatsuoka, F., Tateyama, M., Koseki, J. and Uchimura, T. (1995) Geotextile-reinforced soil retaining wall and their seismic behaviour , Proc. of 10th Asian Regional Conf. on Soil Mechanics and Foundation Engineering, Beijing, 2, 26-49.
Tatsuoka, F., Tateyama M. and Koseki, J. (1996) Performance of soil retaining walls for railway embankments, Soils and Foundations, Special Issue of Soils and Foundations on Geotechnical Aspects of the January 17 1995 Hyogoken-Nambu Earthquake, 311-324.